Heliyon 10 (2024) e36910

Contents lists available at ScienceDirect

Heliyon

journal homepage: www.cell.com/heliyon

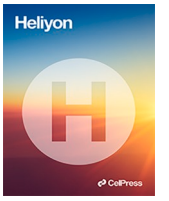

Research article

Sensitive sandwich-type electrochemical immunosensing of p53 protein based on $Ti_3C_2T_x$ MXene nanoribbons and ferrocene/gold

Song Lin, Lixin Wen, Hong Zhao, Donghua Huang, Zuwei Yang, Qinge Zou, Ling Jiang *

Sanming Integrated Medicine Hospital Affiliated to Fujian University of Traditional Chinese Medicine, Sanming, 365000, PR China

ARTICLE INFO

Keywords:
p53 protein
Tumor
Electrochemical immunosensor
MXene
$Ti_3C_2T_x$
Ferrocene

ABSTRACT

Since the p53 protein is an important promising biomarker of lung tumor and colorectal tumor, it is very essential to design a highly effective mean to monitor the degree of p53 for the early clinical analysis/therapy of the related tumors. In this work, a sandwich-type electrochemical immunosensing (SES) platform is proposed for the first time to detect p53 via synthesizing $Ti_3C_2T_x$ MXene nanoribbons ($Ti_3C_2T_x$ Nb) and ferrocene/gold nanoparticles (Fc/Au) respectively as the sensing substrate and signal-amplifier. The superior electrical property and large surface area of $Ti_3C_2T_x$ Nb are beneficial to assemble the initial p53-antibodies (Ab_1), while the synthesized Fc/Au is devoted to assemble the secondary p53 antibodies (Ab_2) and gives a magnified signal. By adopting the Fc molecules as the probes, the experiments reveal the response current of Fc resulted from the SES structure increases along with the p53 increase from 1.0 to 200.0 pg mL^{-1}. A considerable low detection limit (1.0 pg mL^{-1}) is achieved after optimizing several key conditions, it is thus confirmed the as-proposed SES mean exhibits significant application in the detection of p53 protein and other targets.

1. Introduction

The malignant tumors are a kind of diseases with extremely high mortality, generally the early monitor towards the related biomarkers has important significance to offer vital information for the timely and efficient therapy [1–3]. As a reported tumor inhibitor, the p53 protein plays key roles to prevent the gene mutations and maintain the genome integrity [4,5], and generally the physiological degree of p53 in normal human is considerable low (<10 pg mL^{-1}) [6–8]. In such case, the accurate quantification of p53 is extremely useful for the early clinical analysis and therapy of the malignant tumors. Traditional means for the detection of p53 mainly include enzyme-linked immunosorbent assay, chromatography-mass spectrometry and western blotting, immunohistochemistry [9–12], but which were restricted resulted from their cost, operation and analysis times. Sequentially significant efforts have been motivated to design low-cost, simple and rapid methodologies. Recently, the electrochemical immunoassays received some attentions since they exhibit some unique superiorities such as simple operation, inexpensive and time-saving [6,13]. In addition, it has been reported, attributed to the advantages in the feature of signal-amplification, the sandwich-type electrochemical immunosensing (SES) means have aroused considerable attentions to detect various analytes in the past years [14–16]. Therefore, it is very promising to design a sensitive and effective SES platform for p53 detection.

* Corresponding author.
E-mail address: JiangLingDoc123456@yeah.net (L. Jiang).

https://doi.org/10.1016/j.heliyon.2024.e36910
Received 2 July 2024; Received in revised form 23 August 2024; Accepted 23 August 2024
Available online 24 August 2024

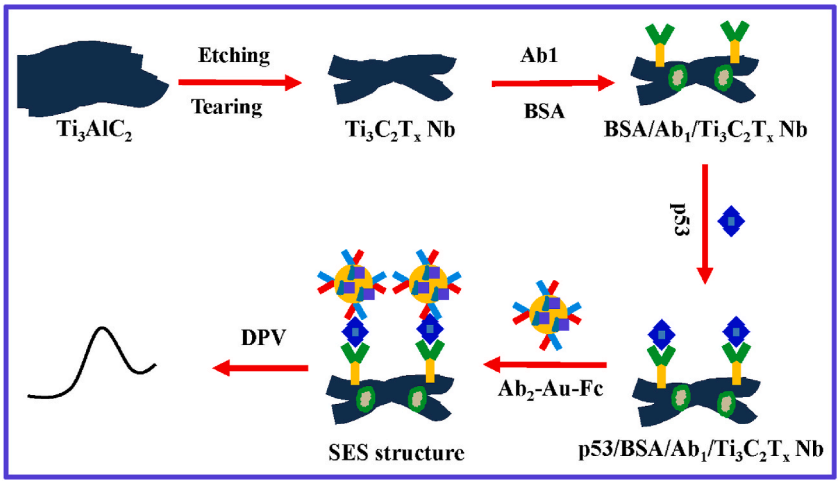

Scheme 1. Illustrations for constructing the as-designed SES sensing platform of p53.

As one of the two key factors in constructing SES platform, designing or selecting appropriate nanomaterial as the substrate of sensor is very important [17–19]. As a type of emerging-representative 2D materials with high electrical conductivity and large surface area recently, the compounds of transition metal carbides/carbonitrides (denoted as MXenes) have been utilized widely in many research fields such as energy storage and conversion, sensors and biomedicine [20–24]. For instance, by growing CoFe-PBA on ferrocene functionalized $Ti_3C_2T_x$ MXene, Wang et al. [25] developed a sensitive electrochemical sensor of xanthine. In this sensor, the introduction of $Ti_3C_2T_x$ MXene is dedicated to accommodate ferrocene and give higher conductivity. In general, MXenes are achieved by exfoliating the "A" element in the MAX phase, where "M" is the transition metal and "A" is the element in the IIIA/IVA group, while "X" refers to C or/and N [26–28]. In addition, the MXenes-based nanomaterials can offer good biocompatibility and be easy to functionalizing. These superiorities of MXenes devoted themselves to be a desirable candidate as the substrate to construct a SES platform for p53. In addition, there is no doubt the construction of signal amplifier is also considerable important for the sensing performances of SES platform. Nanogold (Au), as an universally accessible precious metal exhibiting superior conductivity and biocompatibility, is very easy to be functionalized [29,30]. Meanwhile, the ferrocene (Fc) molecule is a common and acceptable signal-probe since it can exhibit high electroactivity [31,32].

Inspired by the above insights, in this work, by synthesizing $Ti_3C_2T_x$ MXene (a typical MXene material) nanoribbons ($Ti_3C_2T_x$ Nb) as the substrate to assemble Ab_1 of p53 (Ab_1-$Ti_3C_2T_x$ Nb), and functionalizing Fc coupled with Ab_2 of p53 to the Au surface as the specific signal-amplifier (Ab_2-Au-Fc), we proposed a novel SES mean to detect the degree of p53 (Scheme 1). In the existence of p53 protein, a SES structure consisted of Ab_2-Au-Fc/p53/Ab_1-$Ti_3C_2T_x$ Nb would be formed and the relative response signal of the Fc probe is proportional and sensitive to the p53 level, hence achieving a highly sensitive and effective monitoring for the p53 protein. This works provided a reliable and sensitive mean for p53 detection, it's expected which can offer significant real application.

2. Experimental section

2.1. Reagents and equipment

The Ti_3AlC_2 raw material was purchased from Forsman Technology Company (China). HF (≥40.0 %), KOH, $HAuCl_4{\cdot}3H_2O$, $NaBH_4$, Fc, NaOH, 4-aminobenzoic acid (PABA), 4-aminobenzoic acid (ABZ) 1-Ethyl-3-[3-dimethylaminopropyl]carbodiimide hydrochloride (EDC), $NaNO_2$ and N-hydroxysuccinimide (NHS) were obtained from Aladdin Biotechnology Co., Ltd (China). Bovine serum albumin (BSA), carcinoembryonic antigen (CEA), alpha fetoprotein (AFP), IgG antigen and anti-p53 antibodies were offered by Abcam Co., Ltd. The phosphate buffer solution (PBS) were prepared with KH_2PO_4 (0.1 M), K_2HPO_4 (0.1 M) and KCl (0.1 M). Electrochemical CHI 660E Workstation was utilized for all the electrochemical measurements.

2.2. Synthesization of $Ti_3C_2T_x$ Nb

The $Ti_3C_2T_x$ MXene nanosheets ($Ti_3C_2T_x$ NS) were firstly synthesized via etching the Al layer in the Ti_3AlC_2 powder according to the reported method [33]. Briefly, under stirring at ~35 °C, 05 g raw material of Ti_3AlC_2 was slowly added into a HF solution of 10.0 mL. After holding for 20 h, the $Ti_3C_2T_x$ NS can be obtained via washing and drying.

Next, $Ti_3C_2T_x$ Nb were synthesized via tearing the above obtained $Ti_3C_2T_x$ NS as follows: the 0.1 g $Ti_3C_2T_x$ NS were added into a 3.0 M KOH solution (25.0 mL) under continuous stirring under for 2 days at room temperature, thus the designed $Ti_3C_2T_x$ Nb can be collected after washing and drying. For further functionalizing $Ti_3C_2T_x$ Nb with carboxyl dedicated to immobilize Ab_1, 0.08 g ABZ and 0.07g NaOH were firstly added to 25.0 mL watery. Next, 3.0 mL HCl solution was added quickly to the solution and maintained for

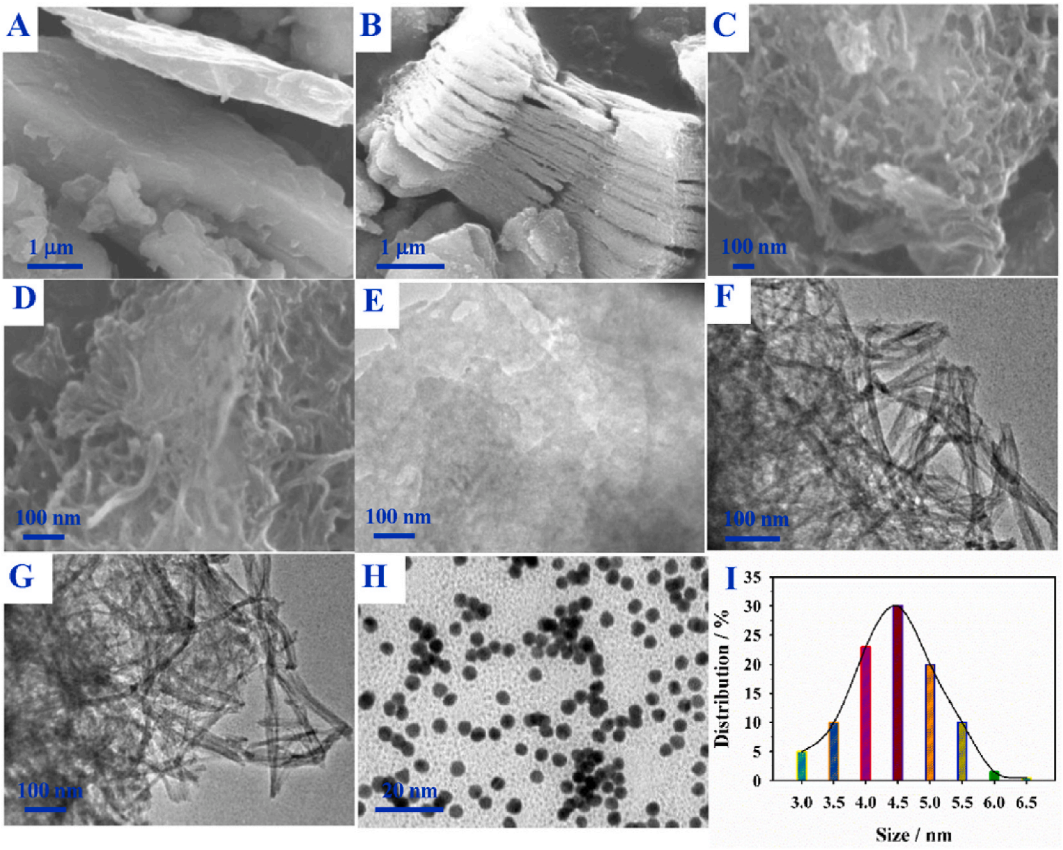

Fig. 1. The SEM images of (A) Ti_3AlC_2, (B) $Ti_3C_2T_x$ NS, (C) $Ti_3C_2T_x$ Nb and (D) carboxylated $Ti_3C_2T_x$ Nb; the TEM images of (E) $Ti_3C_2T_x$ NS, (F) $Ti_3C_2T_x$ Nb, (G) carboxylated $Ti_3C_2T_x$ Nb and (H) Au particles; (I) the particle size distribution of Au.

~30 min under stirring. In final, the formed mixture were centrifuged and dried to achieve $Ti_3C_2T_x$ Nb product.

2.3. Synthesization for Au and immobilizing Ab_2 coupled with Fc

For preparing Ab_2-Au-Fc, the tiny Au nanoparticles were firstly synthesized: 0.1 mL sodium citrate solution (0.2 M) was added dropwise to a 3.0 mL $HAuCl_4$ solution and heated at about 60 °C for 2 h, thus obtaining the Au nanoparticles. Then, 20.0 μL Ab_2 solution of 60.0 μg mL^{-1} and 20.0 μL Fc solution of 0.4 mM were added into the obtained Au solution (1.0 mL), and this mixture was incubated for 1 h at room temperature to obtain Ab_2-Au-Fc signaling amplifier.

2.4. Fabrication of the SES structure

Firstly, a definite of $Ti_3C_2T_x$ Nb suspension of (1.0 mg mL^{-1}) was dropped to the surface of SPCE electrode and a 1:1 mixture solution containing EDC/NHS (0.1 M/0.2 M) were used to activate carboxyls. In sequentially, 8.0 μL solution of Ab_1 (10.0 μg mL^{-1}) was coated and immobilized to the activated surface of $Ti_3C_2T_x$ Nb/SPCE as Ab_1/$Ti_3C_2T_x$ Nb/SPCE. Then, 3.0 μL BSA (100.0 mg mL^{-1}) was utilized to restrict the non-specific immobilization. For sensing p53, the fabricated BSA/Ab_1/$Ti_3C_2T_x$ Nb/SPCE was interacted with p53 at various degrees, and a SES structure would be formed by combining p53/BSA/Ab_1/$Ti_3C_2T_x$ Nb/SPCE with Ab_2-Au-Fc, which was then monitored via differential pulse voltammetry (DPV).

3. Results and discussion

3.1. Characterization of the synthesized $Ti_3C_2T_x$ Nb and Au

Fig. 1 displayed the SEM and TEM images of the as-synthesized $Ti_3C_2T_x$ Nb and related materials. It was noted the original Ti_3AlC_2 materials show smooth surface with aligned densely layered-structures (Fig. 1A). After HF etching, the synthesized $Ti_3C_2T_x$ NS (Fig. 1B and E) layered-structures were very evident and displayed packed loosely accordion-type morphology compared to the original Ti_3AlC_2 sample. Interestingly, via tearing $Ti_3C_2T_x$ NS, $Ti_3C_2T_x$ Nb (Fig. 1C and F) could be well evidenced with minor diameter (~28

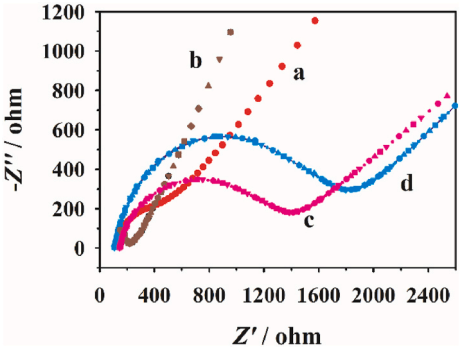

Fig. 2. The EIS plots of SPCE (a), $Ti_3C_2T_x$ Nb/SPCE (b), BSA/Ab_1/$Ti_3C_2T_x$ Nb/SPCE (c), and Ab_2-Au-Fc/p53/BSA/Ab_1/$Ti_3C_2T_x$ Nb/SPCE (d).

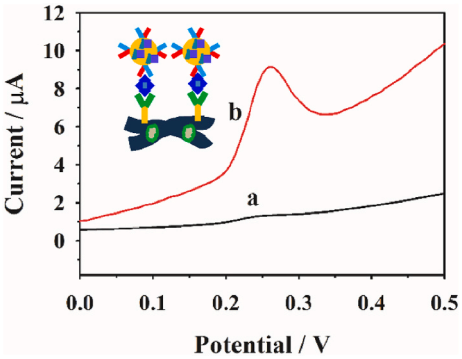

Fig. 3. DPV response of (a) BSA/Ab_1/$Ti_3C_2T_x$ Nb/SPCE and (b) p53/BSA/Ab_1/$Ti_3C_2T_x$ Nb/SPCE after their incubation in Ab_2-Au-Fc solution.

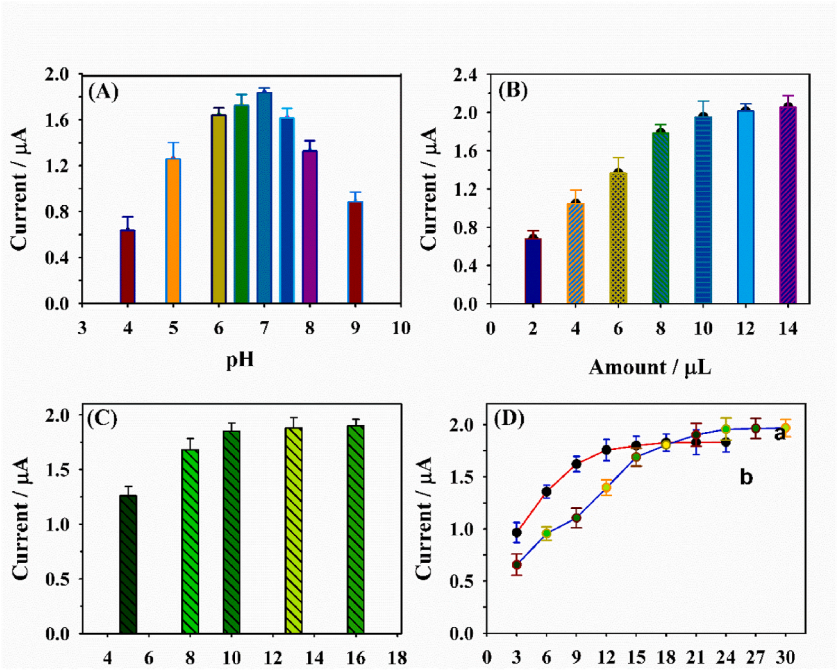

Fig. 4. Influences of the (A) pH value of PBS; (B) amount of $Ti_3C_2T_x$ Nb; (C) Ab_1 concentration; (D) interaction time of p53 with BSA/Ab_1/$Ti_3C_2T_x$ Nb (a) and p53/BSA/Ab_1/$Ti_3C_2T_x$ Nb with Ab_2-Au-Fc (b).

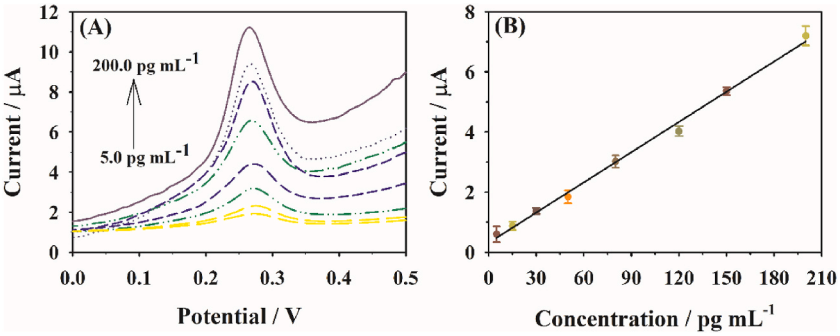

Fig. 5. (A) The DPV responses of p53 with various concentrations (5.0, 15.0, 30.0, 50.0, 80.0, 120.0, 150.0 and 200.0 pg mL^{-1}) based on the developed SES sensor; (B) the calibration plot of p53 detection.

Table 1
Comparisons of various immunosensing platform with the present method for p53 protein.

Electrode	Method	Linearity (pg mL^{-1})	LOD (pg mL^{-1})	Ref.
AuNPs	LSV	87000.0–2100000.0	2100.0	[5]
PEDOT:PSS/AuNPs	DPV	1000.0–120000.0	90.0	[4]
Au/NiPc	DPV	0.1–500.0	–	[34]
SAM	LSV	4.3–4370.0	4.3	[35]
PEG	CV	10.0–10000.0	10.0	[36]
PTAA/Au/PMB	SWV	1000.0–100000.0	650.0	[37]
$Ti_3C_2T_x$ Nb	DPV	5.0–200.0	1.0	This work

* PEDOT:PSS (poly (3, 4-ethylenedioxythiophene):polystyrenesulfonate); NiPc: nickel phthalocyanine; SAM: Self-assembled monolayer; PEG: pencil graphite electrode; PTAA: poly(thiophene acetic acid); PMB: poly(thiophene acetic acid); LSV: linear sweep voltammograms; CV: cyclic voltammetry; SWV: square wave voltammetry.

nm). As is evident, the $Ti_3C_2T_x$ Nb with carboxyl groups have well-defined structures that were almost the same as displayed for $Ti_3C_2T_x$ Nb (Fig. 1D and G). This indicates that the carboxyl functionalization does not change the microstructure and morphology of the materials, thus which were further characterized by Fourier transform infrared (FT-IR) spectrum (Fig. S1). Compared with the pure $Ti_3C_2T_x$ Nb, the carboxylated $Ti_3C_2T_x$ Nb gave a strong and typical peak of the carboxyl at ~1637 cm^{-1}.

Next, the used Au particles were characterized by TEM. As shown in Fig. 1H and I, the as-synthesized Au nanoparticles exhibited very uniform size, and the diameter is tiny to about 4.5 nm through statistical investigation, such small size is beneficial to immobilize Ab_2 and Fc molecules.

3.2. Electrochemical evaluation of the SES platform

The impedance spectroscopy (EIS) was firstly utilized to characterize the processes in fabricating SES structure, which was conducted in a $[Fe(CN)_6]^{3-/4-}$ solution (5.0 mM) (Fig. 2). In general, the common biomolecules exhibit poor conductive and pose inhibiting effect to the electron channel, thus increasing the impedance values. As displayed in Fig. 2, the charge-transfer resistance (R_{CT}) of $Ti_3C_2T_x$ Nb/SPCE was smaller compared to the bare SPCE resulted from the superior conductivity of the $Ti_3C_2T_x$ MXene. When Ab_1, p53 and Ab_2-Au-Fc were assembled in successive to the surface of $Ti_3C_2T_x$ Nb/SPCE, the R_{CT} values at the fabricated BSA/Ab_1/$Ti_3C_2T_x$ Nb/SPCE and Ab_2-Au-Fc/p53/BSA/Ab_1/$Ti_3C_2T_x$ Nb/SPCE showed an increase in turn. These indicated that the fabricated SES layer was achieved successfully.

The feasibility about the as-proposed SES sensor was characterized by DPV technology as it can offer superior sensitivity. Fig. 3 displayed the DPV curves of BSA/Ab_1/$Ti_3C_2T_x$ Nb/SPCE and p53/BSA/Ab_1/$Ti_3C_2T_x$ Nb/SPCE after the incubation with Ab_2-Au-Fc. The achieved results revealed there is no DPV signal presented without p53 (300.0 pg mL^{-1}), that is BSA/Ab_1/$Ti_3C_2T_x$ Nb/SPCE. Nevertheless, a strong DPV current of Fc could be noted at p53/BSA/Ab_1/$Ti_3C_2T_x$ Nb/SPCE after incubating with Ab_2-Au-Fc to generate a SES structure (Ab_2-Au-Fc/p53/BSA/Ab_1/$Ti_3C_2T_x$ Nb). The related reason was that the specific antibody-antigen recognition between p53-antibodies and p53 could induce the Ab_2-Au-Fc capture to p53/BSA/Ab_1/$Ti_3C_2T_x$ Nb. These suggested that the as-proposed SES proposal for p53 was feasible.

In order to achieve the sensitive determination for p53, several key experiments need to be optimized. Firstly, there is no doubt that the acid-base property of sensing system is very important. Fig. 4A gave the effect of the different pH values of PBS to the DPV signal of Ab_2-Au-Fc/p53/BSA/Ab_1/$Ti_3C_2T_x$ Nb/SPCE, it's noted the signals increased along with the pH value increase and the maximum was at 7.0. As for the influence from the dropped amount of $Ti_3C_2T_x$ Nb to the surface of electrode (Fig. 4B), the peak current increases with the amount increase. Whereas when exceeding 10.0 μL, the DPV signal showed little change, so 10.0 μL $Ti_3C_2T_x$ Nb dispersion was the amount that coated to the SPCE surface. Meanwhile, Fig. 4C exhibited the effect of Ab_1 concentration, the results revealed 10.0 μg

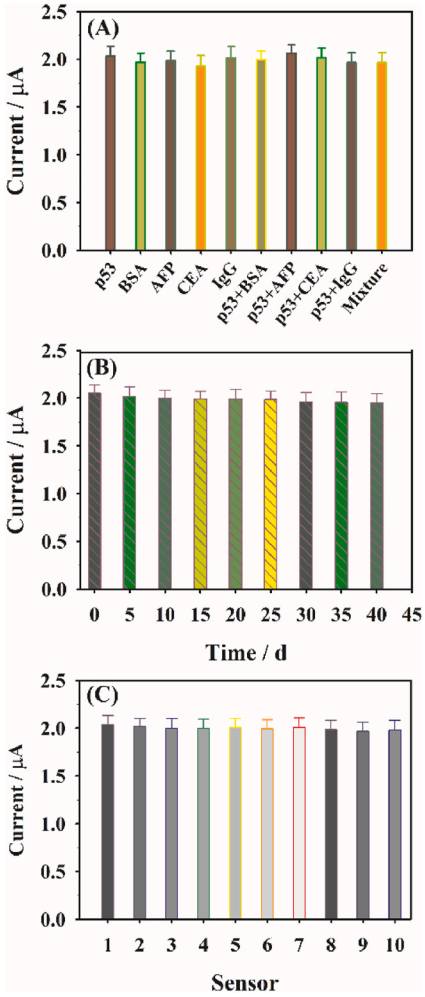

Fig. 6. (A) Selectivity, (B) reproducibility and (C) stability for p53 detection based on the constructed SES sensor.

mL^{-1} is enough, thus this concentration was used for the experiments. Fig. 4D displayed the effect about the interaction time between p53 and its antibodies. It can be found the desirable time between p53 and Ab_1 was 12 min, while that was 21 min between p53 and Ab_2.

Finally, the detection capabilities of the as-fabricated SES mean for p53 were evaluated. As displayed in Fig. 5, the DPV signals gradually increased with the p53 level increased ranging from 5.0 to 200.0 pg mL^{-1} (Fig. 5A), and the linear equation can be written down as $\Delta I\ (\mu A) = 0.314 + 0.034C$ (pg mL^{-1}) (Fig. 5B). Based on S/N = 3, the limit of detection (LOD) was 1.0 pg mL^{-1}. In order to further understand the as-designed SES mean, the comparisons between this work and other sensors for p53 detection were also performed. From Table 1, it was assured the detection performances of the SES mean were comparable to the previous immunosensors with lower LOD value. In addition, it should be pointed out that the p53 protein can be divided into wild type and mutant type. The wild-type p53 protein is extremely unstable, with a half-life of only a few minutes, while the mutant p53 proteins are more stable, have a longer half-life. Therefore, the p53 protein detected by this sensor is mutant p53 protein.

3.3. Reliability and real samples analysis

Firstly, the proposed SES mean's selectivity was confirmed after the addition of various interfering substances to the detection system. As displayed in Fig. 6A, it was observed there was little change observed for the signal of Fc after the addition of BSA, AFP, CEA and IgG (10.0 times of p53 level). The stability of the SES mean was also evaluated (Fig. 6B), and the signal responses of SES structure remained almost unchanged via storing the sensing platform for 40 days. Next, the reproducibility was investigated by measuring the signals of Fc at 10-independently-fabricated SES structures. As displayed in Fig. 6C, the RSD value between them was 3.68 %. These indicated the as-fabricated SES mean exhibited desirable reliability.

Finally, the standard addition technique was adopted to validate the as-proposed SES mean in real application. Various degrees of p53 protein were added in turn to the real human serum samples, and the response signals of the SES sensor towards these samples

were recorded. Then, the recoveries were calculated to reveal the capability in the real applications. From Table S1, the obtained recoveries were ranging from 94.7 % to 97.0 %, confirming the as-proposed SES sensing platform exhibited satisfactory real ability for p53 detection.

4. Conclusion

In summary, a novel SES sensing platform for p53 was designed in this work by preparing $Ti_3C_2T_x$ Nb as sensing platform and Au particles to immobilize Fc and Ab_2 as signal amplifier. Owing to the excellent properties (e.g., high electrical conductivity and large surface area) of $Ti_3C_2T_x$ Nb which are beneficial to immobilize Ab_1 and improve conductivity, and the signal amplification function of Ab_2-Au-Fc, the as-designed SES sensing platform displayed superior analytical performances under the optimized conditions: wider linearity (5.0–200.0 pg mL^{-1}) coupled with lower LOD (1.0 pg mL^{-1}). Additionally, the as-proposed SES mean displayed good stability, selectivity and reproducibility as well as real applications, suggesting this SES mean for p53 showed important potential application. Through adopting other appropriate antibodies instead of p53 antibodies, we expected the as-designed SES sensing model has a broad application in the detection for other analytes.

Data availability statement

Data will be made available on request.

CRediT authorship contribution statement

Song Lin: Writing – original draft, Visualization, Validation, Methodology, Investigation, Data curation. **Lixin Wen:** Writing – review & editing, Validation, Supervision, Software, Resources. **Hong Zhao:** Writing – review & editing, Validation, Resources, Data curation. **Donghua Huang:** Validation, Resources, Methodology. **Zuwei Yang:** Validation, Investigation. **Qinge Zou:** Data curation, Conceptualization. **Ling Jiang:** Writing – review & editing, Validation, Supervision, Project administration, Methodology, Investigation, Funding acquisition.

Declaration of competing interest

The authors declare that they have no known competing financial interests or personal relationships that could have appeared to influence the work reported in this paper.

Acknowledgment

This work was financially supported by Fujian Province Natural Science Foundation (No.: 2023J011759).

Appendix A. Supplementary data

Supplementary data to this article can be found online at https://doi.org/10.1016/j.heliyon.2024.e36910.

References

[1] E.B. Aydın, M. Aydın, M.K. Sezgintürk, Electrochemical immunosensor based on chitosan/conductive carbon black composite modified disposable ITO electrode: an analytical platform for p53 detection, Biosens. Bioelectron. 121 (2018) 80–89.
[2] A.F. Cruz-Pacheco, J. Quinchia, J. Orozco, Cerium oxide–doped PEDOT nanocomposite for label-free electrochemical immunosensing of anti-p53 autoantibodies, Microchim. Acta 189 (2022) 228.
[3] J. Zhao, A. Blayney, X. Liu, L. Gandy, W. Jin, L. Yan, J.-H. Ha, A.J. Canning, M. Connelly, C. Yang, EGCG binds intrinsically disordered N-terminal domain of p53 and disrupts p53-MDM2 interaction, Nat. Commun. 12 (2021) 986.
[4] J. Kang, Z. Li, G. Wang, A novel signal amplification strategy electrochemical immunosensor for ultra-sensitive determination of p53 protein, Bioelectrochemistry 137 (2021) 107647.
[5] O. Amor-Gutiérrez, E. Costa-Rama, N. Arce-Varas, C. Martínez-Rodríguez, A. Novelli, M.T. Fernández-Sánchez, A. Costa-García, Competitive electrochemical immunosensor for the detection of unfolded p53 protein in blood as biomarker for Alzheimer's disease, Anal. Chim. Acta 1093 (2020) 28–34.
[6] A.F. Cruz-Pacheco, J. Quinchia, J. Orozco, Nanostructured poly (thiophene acetic acid)/Au/poly (methylene blue) interface for electrochemical immunosensing of p53 protein, Microchim. Acta 190 (2023) 136.
[7] C.-X. Yu, F. Xiong, L.-L. Liu, Electrochemical biosensors for the detection of p53 proteins and anti-p53 autoantibody, Int. J. Electrochem. Sci. 15 (2020) 6695–6705.
[8] J.L. Silva, E.A. Cino, I.N. Soares, V.F. Ferreira, G. AP de Oliveira, Targeting the prion-like aggregation of mutant p53 to combat cancer, Accounts Chem. Res. 51 (2018) 181–190.
[9] L. Chen, J. Liang, A proximity ligation assay (PLA) based sensing platform for the ultrasensitive detection of P53 protein-specific SUMOylation, Process Biochem. 112 (2022) 1–5.
[10] L. Liang, L. Jin, Y. Ran, L.-P. Sun, B.-O. Guan, Fiber light-coupled optofluidic waveguide (FLOW) immunosensor for highly sensitive detection of p53 protein, Anal. Chem. 90 (2018) 10851–10857.

[11] E. Assah, W. Goh, X.T. Zheng, T.X. Lim, J. Li, D. Lane, F. Ghadessy, Y.N. Tan, Rapid colorimetric detection of p53 protein function using DNA-gold nanoconjugates with applications for drug discovery and cancer diagnostics, Colloids Surf. B Biointerfaces 169 (2018) 214–221.
[12] Y. Xia, L. Wu, Y. Hu, Y. He, Z. Cao, X. Zhu, X. Yi, J. Wang, Sensitive surface plasmon resonance detection of methyltransferase activity and screening of its inhibitors amplified by p53 protein bound to methylation-specific ds-DNA consensus sites, Biosens. Bioelectron. 126 (2019) 269–274.
[13] V. Ostatná, H. Černocká, T. Galicová, S. Hasoň, Electrochemical analysis of proteins important in cancer. Behavior of anterior gradient receptors, p53 protein and their complexes at charged surfaces, Curr. Opin. Electrochem. (2023) 101269.
[14] X. Lin, P.P. Liu, J. Yan, D. Luan, T. Sun, X. Bian, Dual synthetic receptor-based sandwich electrochemical sensor for highly selective and ultrasensitive detection of pathogenic bacteria at the single-cell level, Anal. Chem. 95 (2023) 5561–5567.
[15] G. Kim, H. Cho, P. Nandhakumar, J.K. Park, K.-S. Kim, H. Yang, Wash-free, sandwich-type protein detection using direct electron transfer and catalytic signal amplification of multiple redox labels, Anal. Chem. 94 (2022) 2163–2171.
[16] H. Zhang, Z. Lin, Y. Li, Z. Lin, S. Yang, B. Qiu, M. Yu, Highly sensitive detection of thyroglobulin based on sandwich-type electrochemical immunoassay, Anal. Sci. 39 (2023) 969–975.
[17] J. Chen, P. Tong, L. Huang, Z. Yu, D. Tang, Ti3C2 MXene nanosheet-based capacitance immunoassay with tyramine-enzyme repeats to detect prostate-specific antigen on interdigitated micro-comb electrode, Electrochim. Acta 319 (2019) 375–381.
[18] Z. Wang, H. Zhao, K. Chen, S. Cao, M. Lan, Sandwich-type electrochemical aptasensor based on HMCS@ PDA@ AuNPs and PtCu DNs/MUN-CuO-TiO2 for ultrasensitive detection of cardiac troponin I, Sensor. Actuator. B Chem. 393 (2023) 134275.
[19] S. Lin, J. Wang, X. Wang, S. Xia, L. Wu, Simple and sensitive sandwich-like electrochemical immunosensing strategy for D-dimer based on cyclodextrin-carbon nanotube and nanogold-ferrocene, Heliyon 10 (2024) e28793.
[20] M. Mohammadniaei, A. Koyappayil, Y. Sun, J. Min, M.-H. Lee, Gold nanoparticle/MXene for multiple and sensitive detection of oncomiRs based on synergetic signal amplification, Biosens. Bioelectron. 159 (2020) 112208.
[21] F. Cao, Y. Zhang, H. Wang, K. Khan, A.K. Tareen, W. Qian, H. Zhang, H. Ågren, Recent advances in oxidation stable chemistry of 2D MXenes, Adv. Mater. 34 (2022) 2107554.
[22] P.K. Kalambate, Dhanjai, A. Sinha, Y. Li, Y. Shen, Y. Huang, An electrochemical sensor for ifosfamide, acetaminophen, domperidone, and sumatriptan based on self-assembled MXene/MWCNT/chitosan nanocomposite thin film, Microchim. Acta 187 (2020) 402.
[23] F. Liu, L. Han, Y. Yang, Z. Xue, X. Lu, X. Liu, Designable synthesis of a novel layered MXene loaded gold nanocluster composite for efficient electrochemical sensing of homocysteine in biological samples, Chem. Eng. J. 461 (2023) 141928.
[24] T. Liu, R. Zhou, K. Wu, G. Zhu, Colorimetric method transforms into highly sensitive homogeneous voltammetric sensing strategy for mercury ion based on mercury-stimulated Ti3C2Tx MXene nanoribbons@ gold nanozyme activity, Anal. Chim. Acta 1250 (2023) 340975.
[25] M. Chu, Y. Wang, J. Xin, L. Zhang, Y. Liu, G. Yang, H. Ma, Y. Wang, H. Pang, X. Wang, In situ growth of CoFe-prussian blue analog nanospheres on ferrocene-functionalized ultrathin layered $Ti_3C_2T_x$ MXene frameworks for efficient detection of xanthine, Chem. Eng. J. 469 (2023) 143866.
[26] X. Tu, F. Gao, X. Ma, J. Zou, Y. Yu, M. Li, F. Qu, X. Huang, L. Lu, Mxene/carbon nanohorn/β-cyclodextrin-Metal-organic frameworks as high-performance electrochemical sensing platform for sensitive detection of carbendazim pesticide, J. Hazard Mater. 396 (2020) 122776.
[27] H. Zhang, Z. Wang, F. Wang, Y. Zhang, H. Wang, Y. Liu, In situ formation of gold nanoparticles decorated Ti3C2 MXenes nanoprobe for highly sensitive electrogenerated chemiluminescence detection of exosomes and their surface proteins, Anal. Chem. 92 (2020) 5546–5553.
[28] D. Wang, C. Zhou, A.S. Filatov, W. Cho, F. Lagunas, M. Wang, S. Vaikuntanathan, C. Liu, R.F. Klie, D.V. Talapin, Direct synthesis and chemical vapor deposition of 2D carbide and nitride MXenes, Science 379 (2023) 1242–1247.
[29] S. Han, W. Liu, M. Zheng, R. Wang, Label-free and ultrasensitive electrochemical DNA biosensor based on urchinlike carbon nanotube-gold nanoparticle nanoclusters, Anal. Chem. 92 (2020) 4780–4787.
[30] T. Yu, Y. Fu, J. Yi, Z. Wang, J. Zhang, Y. Xianyu, Sulfhydryl-mediated etching suppression of gold nanostars for rapid and sensitive detection of bacterial pathogens, Chem. Eng. J. 481 (2024) 148650.
[31] B. Wu, S. Yeasmin, Y. Liu, L.-J. Cheng, Sensitive and selective electrochemical sensor for serotonin detection based on ferrocene-gold nanoparticles decorated multiwall carbon nanotubes, Sensor. Actuator. B Chem. 354 (2022) 131216.
[32] W. Lee, L. Li, M. Camarasa-Gómez, D. Hernangómez-Pérez, X. Roy, F. Evers, M.S. Inkpen, L. Venkataraman, Photooxidation driven formation of Fe-Au linked ferrocene-based single-molecule junctions, Nat. Commun. 15 (2024) 1439.
[33] H. Wu, M. Almalki, X. Xu, Y. Lei, F. Ming, A. Mallick, V. Roddatis, S. Lopatin, O. Shekhah, M. Eddaoudi, H.N. Alshareef, MXene derived metal-organic frameworks, J. Am. Chem. Soc. 141 (2019) 20037–20042.
[34] Y.-J. Chen, Y.-R. Peng, H.-Y. Lin, T.-Y. Hsueh, C.-S. Lai, M.-Y. Hua, Preparation and characterization of Au/NiPc/Anti-p53/BSA electrode for application as a p53 antigen sensor, Chemosensors 9 (2021) 17.
[35] L. Hou, Y. Huang, W. Hou, Y. Yan, J. Liu, N. Xia, Modification-free amperometric biosensor for the detection of wild-type p53 protein based on the in situ formation of silver nanoparticle networks for signal amplification, Int. J. Biol. Macromol. 158 (2020) 580–586.
[36] B. Nohwal, R. Chaudhary, C. Pundir, Amperometric detection of tumor suppressor protein p53 via pencil graphite electrode for fast cancer diagnosis, Anal. Biochem. 639 (2022) 114528.
[37] A.F. Cruz-Pacheco, J. Quinchia, J. Orozco, Nanostructured poly(thiophene acetic acid)/Au/poly(methylene blue) interface for electrochemical immunosensing of p53 protein, Microchim. Acta 190 (2023) 136.